



**Analysis of Mesh-Based Neutron Source Models
for Better Coupling of Plasma Physics and
Neutronics**

R.N. Slaybaugh, P.P.H. Wilson, L.A. El-Guebaly, E.P. Marriott

January 2009

UWFDM-1343

Published in *Fusion Engineering and Design* 84, Issues 7-11 (June 2009) 1774-1778.

FUSION TECHNOLOGY INSTITUTE
UNIVERSITY OF WISCONSIN
MADISON WISCONSIN

**Analysis of Mesh-Based Neutron Source
Models for Better Coupling of Plasma Physics
and Neutronics**

R.N. Slaybaugh, P.P.H. Wilson, L.A. El-Guebaly, E.P. Marriott

Fusion Technology Institute
University of Wisconsin
1500 Engineering Drive
Madison, WI 53706

<http://fti.neep.wisc.edu>

January 2009

UWFDM-1343

Published in *Fusion Engineering and Design* 84, Issues 7-11 (June 2009) 1774-1778.

Abstract

Developments in computer architecture and neutronics code capabilities have enabled high-resolution analysis of complex 3-D geometries. Thus, accurately modeling 3-D source distributions has become important for performing nuclear analyses. In this work two methods are described which generate and sample such 3-D sources based directly on the plasma parameters of a fusion device and which facilitate the ability to update the neutron source following changes to the plasma physics configuration. The cylindrical mesh method is useful for toroidally symmetric machines and utilizes data in a standard file format which represents the poloidal magnetic flux on an R-Z grid. The conformal hexahedral mesh method takes plasma physics data generated in an idealized toroidal coordinate system and uses a Jacobian transformation and a functional expansion to generate the source. This work describes each methodology as well as associated test cases. The cylindrical mesh method was applied to ARIES-RS and the conformal hexahedral mesh method was applied to a uniform torus and to ARIES-CS. The results of these test cases indicate that the improved source definitions can have important effects on pertinent engineering parameters, such as neutron wall loading, and they should therefore be used for high-resolution nuclear analyses of all toroidal devices.

1. Introduction

The advent of high fidelity three-dimensional neutronics analysis of complex geometries for fusion energy systems has drawn attention to the need for improved representations of the neutron source distribution. These new analysis methodologies are being enabled by improved simulation tools and are being driven by an increasing desire to couple the results, particularly fine-resolution nuclear heating, to other types of engineering analysis.

Previous analysis methodologies have relied on approximations to the geometry and/or coarse-resolution output quantities and only in some cases were the results strongly dependent on the spatial distribution of the source. For example, when considering nuclear heating in a fusion blanket or shield for a toroidal machine, a one-dimensional approximation in a cylindrical geometry yields suitable results [1], although the source distribution introduces some error in the first few centimeters of the first wall [2].

CAD-based, continuous energy Monte Carlo calculations are being combined with high resolution output to give more detailed understanding of the behavior of neutrons (and the photons they generate) in these systems [3]. As the level of detail in the output increases, effects of the neutron source distribution become more important.

This work explores different representations of the neutron source distributions to capture the spatial variations calculated by plasma physics simulations. As a secondary benefit, these methods will introduce approaches to more closely couple the results of plasma physics simulations as the source term for neutronics analysis to the analysis itself.

Most modern magnetic fusion energy systems, such as tokamaks and spherical tori, exhibit a toroidal symmetry in which the source is distributed uniformly in the toroidal angle and with some variation in the poloidal and radial directions. There are important exceptions, e.g. stellarators, which also need to be accommodated in any general approach to modeling neutron source distributions. For toroidally symmetric machines, two-dimensional plasma physics simulations are typically sufficient, and a standard file format exists to represent the poloidal magnetic flux on an R-Z grid. This is combined with profile data that tabulates the plasma parameters as a function of the poloidal magnetic flux to arrive at the fusion power density and neutron source density using the Bosch-Hale formulation [4]. For such systems a simple quadrilateral grid can be used for sampling the source position in R and Z, and then uniformly sampling in the toroidal angle. Although this approach is not novel [3], in Section 2 this work will compare this approach to other alternatives and introduce the direct coupling to plasma physics simulations.

For more complicated source distributions, the plasma physics simulations are often carried out in an idealized toroidal coordinate system. A Jacobian transformation from the idealized plasma coordinate system to a real-space

cylindrical coordinate system can be expressed by a functional expansion in the idealized poloidal and toroidal angles for each of a discrete set of flux surfaces. By defining a uniform hexahedral grid in the idealized coordinate system and transforming it to the real coordinate system, a structured mesh representation of the neutron source distribution can be generated for use in random sampling of the position of the neutron source. In Section 3, this work will describe the details of generating and sampling this mesh to capture first-order variations in the source distribution.

In both cases, the neutron wall loading distribution (NWL or Γ) will be used as the basis for establishing the importance of these advanced source representations and comparing their accuracy. The NWL is an important measure of the effect of the source distribution since it is more strongly affected by the source than other design parameters. NWL is often used to normalize the magnitude of other engineering responses through the blanket and shielding module.

2. Cylindrical Mesh

The first approach is based on the two-dimensional representation expressed in the community-standard “geqsk” format [5]. Given information from these codes, this method generates a source density distribution on a cylindrical mesh which is used by MCNPX to create the probability density function (PDF) and cumulative distribution function (CDF) for source sampling. This method was applied to the ARIES-RS tokamak [6] and compared to simplified one- and three-region source distributions specified using the general source description available in MCNPX (i.e. the SDEF card) [7]. Following a description of the method, results showing a comparison in the calculated NWL will be presented. The results of the three region source agree well with the results of the new approach. The source computed with the new cylindrical mesh method, hereafter designated the “actual source”, is recommended for more accurate future analysis.

The neutron source density, S , is a function of ion temperature, T_i , and density, n_i , which are defined as functions of the poloidal magnetic flux, ψ , which is in turn defined on an R-Z grid. This information is given as output from the plasma physics simulations, so the expansion itself is not required for this method. Thus,

$$S(R, Z) = S[T_i(R, Z), n_i(R, Z)] = S\{T_i[\psi(R, Z)], n_i[\psi(R, Z)]\}. \quad (1)$$

In addition to the *geqsk* file defining the magnetic flux on the R-Z grid, temperature and density profiles are defined on an arbitrary number of flux surfaces. For each point on the R-Z grid, the magnetic flux is used for a spline

interpolation of the temperature and density profiles and the resultant T_i and n_i are used to calculate the neutron power using the Bosch-Hale formulation. This calculation assigns a value for the source density at each vertex of the cylindrical mesh. The relative probability for each cell, $D_{i,j}$, is computed by integrating the source density over the volume of the mesh cell assuming a linear variation of the source density between adjacent vertices. If indices i,j are used to represent a point (R_i, Z_j) ,

$$D_{i,j} = 2\pi \int_Z dZ \int_r R dR S(R, Z) \approx 2\pi\Delta Z \left[\int_r R dR \left\{ \frac{S(R, Z_{j+1}) + S(R, Z_j)}{2} \right\} \right] \quad (2)$$

$$\bar{S}_{z_i} \equiv \frac{S_{i,j+1} + S_{i,j}}{2} \quad (3)$$

$$\begin{aligned} D_{i,j} &= 2\pi\Delta Z \int_{R_i}^{R_{i+1}} \left(\frac{\bar{S}_{z_{i+1}} - \bar{S}_{z_i}}{R_{i+1} - R_i} (R - R_i) + \bar{S}_{z_i} \right) R dR \\ &= 2\pi\Delta Z \frac{\bar{S}_{z_{i+1}} - \bar{S}_{z_i}}{R_{i+1} - R_i} \left[\left(\frac{R_{i+1}^2}{2} - R_i \cdot R_{i+1} \right) - \left(\frac{R_i^2}{2} - R_i \cdot R_i \right) \right] + \bar{S}_{z_i} (R_{i+1} - R_i) \end{aligned} \quad (4)$$

The PDF, $P_{i,j}$, is found by normalizing these $D_{i,j}$, such that $P_{i,j} = \frac{D_{i,j}}{N}$ and $N = \sum_{i,j} D_{i,j}$, and the CDF is

the cumulative sum of the PDF. To find the source cell a linear search through the CDF is carried out in the Z dimension and then in the R dimension. The location within this cell is sampled uniformly in volume: uniformly in Z and the toroidal angle, and linearly in R. The source is emitted isotropically.

This method was used to compute NWL for an interim design of the ARIES-RS tokamak with a power of 1881.5 MW, a 5.12 m major radius, a 1.28 m minor radius, and a 55 cm magnetic shift. The machine is symmetric about the midplane and the divertor is broken into three regions: an inner plate, an outer plate, and dome [6]. Analysis of this power plant was originally done in 1996, comparing the NWL distribution from a source modeled as three uniform regions to that of a source modeled as a single uniform region. The source was specified using MCNP's general source capability (SDEF) and the three regions were weighted to represent the real source distribution [6]. Figure 1 shows the three region source and first wall; the one region source is comprised of the three regions combined into one. The segmenting around the inner wall allowed for the NWL to be computed with a resolution consistent with the 1996 analysis. This work compares the NWL calculated with the one region uniform source, the three region weighted source, and the cylindrical mesh.

The peak NWL (Γ) values for the inboard, outboard, and the average $\bar{\Gamma}$ are given in Table 1 for each source type. The average is calculated by taking the area-weighted average of the NWL values on each segment.

Table 1. Comparison of results from three source types for ARIES-RS neutron wall loading

	One Uniform Region	Three Uniform Regions	Actual Distribution
Peak Inboard Γ	3.2 MW/m ²	3.8 MW/m ²	4.1 MW/m ²
Peak Outboard Γ	4.8 MW/m ²	5.3 MW/m ²	5.3 MW/m ²
Average Γ	3.1 MW/m ²	3.1 MW/m ²	3.1 MW/m ²

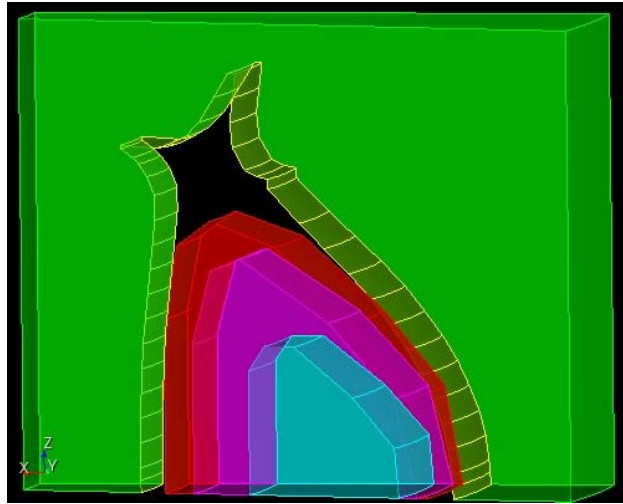


Figure 1. ARIES-RS geometry illustrating the three region source and the inner wall segmenting.

Comparing this to the simple machine average Γ , which is (neutron power)/(first wall area including the divertor), provides a confirmation that the different methods have the same absolute normalization.

For the outboard and divertor cases, the three region source matched the actual source quite well. For the inboard case the three region source was about 8% lower at the midplane, had shallower curvature, and was ~10% higher near the top and the bottom than the actual source, as can be seen in Figure 2. These results indicate that the actual distribution should be used for future analysis because the three region source slightly underpredicted the peak inboard NWL, resulting in underprediction of radiation damage and neutron power deposition.

3. Conformal Hexahedral Mesh

For systems in which the neutron source density varies in all three dimensions, a more complex source representation is necessary. If the plasma physics simulation is simplified by solving on an idealized toroidal coordinate system, it is necessary to provide a Jacobian transformation to the real coordinate system. One common representation of this Jacobian transformation uses a functional expansion, such as the functional expansion for ARIES-CS [8] where the data are output from the plasma physics simulation in a complex set of coefficients [9].

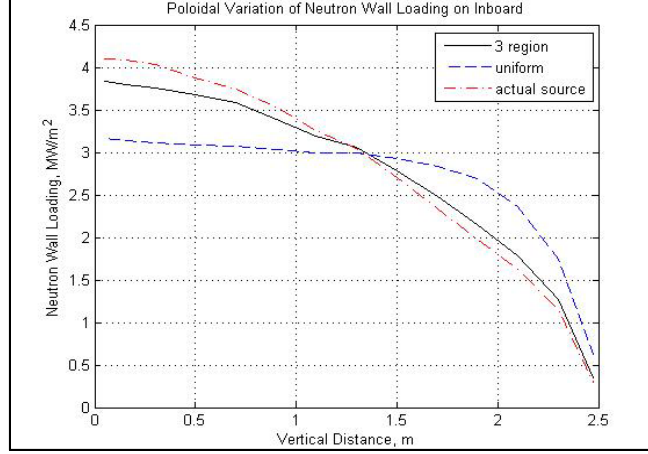


Figure 2. Inboard neutron wall loading results vs. vertical distance.

The coefficients can be transformed into cylindrical coordinates (r,z,ϕ) using Equations 5-7; m is the poloidal and n is the toroidal Fourier mode [10].

$$r(\theta, \phi, s) = \sum_m \sum_n R_{m,n,s} \cos(a_m \theta - a_n \phi) \quad (5)$$

$$z(\theta, \phi, s) = \sum_m \sum_n R_{m,n,s} \sin(a_m \theta - a_n \phi) \quad (6)$$

$$\phi(\theta, \phi, s) = \phi \quad (7)$$

In this section a methodology is developed to use the expansion coefficients to define the source on a set of known flux surfaces. Then, through a process of meshing, coordinate transformation, and numerical integration a source PDF is computed and its corresponding CDF can be sampled for Monte Carlo transport. The method can capture first-order variation of the source distribution within each hex. First the method will be discussed, and then the results of application to two test problems will be presented.

Instead of an R-Z grid in real space, this method begins with a structured hexahedral mesh (hex-mesh) in the idealized toroidal coordinate system of magnetic flux surface, ψ , poloidal angle, θ , and toroidal angle, ϕ . A set of expansion coefficients is provided on a discrete set of flux surfaces, $\{\psi_i\}$, so the hex-mesh should be defined on these same points to avoid additional interpolations and maximize the accuracy of the methodology. These coefficients are used to transform this to an (R,Z,ϕ) cylindrical mesh in real space as discussed above. Although it may be distorted, because the hex-mesh is structured it is straightforward to determine the value of the magnetic flux, ψ , at each vertex in the mesh and to use that to determine the ion temperature, T_i , and density, n_i , based on profiles

similar to those described in the previous section. Again using the Bosch-Hale formulation with these plasma parameters, the source density at each mesh vertex can be determined.

As with the cylindrical mesh methodology above, the source must now be integrated over each hex to arrive at the relative probability. Due to the mesh distortion, it is helpful to borrow from standard finite-element approaches to accomplish both the integration and, later, the random sampling in space [9]. Each hex is mapped onto the so-called natural coordinate system, (ξ, η, ζ) , which is an idealized hexahedron on $[(-1, -1, -1), (1, 1, 1)]$, using shape functions (N_a). The average source at each vertex is then found by numerical integration using a six-node Gaussian quadrature. The process for mapping the coordinates and source values to any point in natural space is detailed in equations 8-10, where $\vec{\xi}$ are the (ξ, η, ζ) coordinates of that point in natural space and a subscript of a or l refers to the a^{th} vertex or the l^{th} quadrature point, respectively.

The values of x, y, z , or the source density, S , at any point (ξ, η, ζ) can be found in a similar manner to the following calculation of x :

$$x(\vec{\xi}) = \sum_{a=1}^8 N_a(\vec{\xi}) x_a^e \quad (8)$$

$$x_a^e = x(\vec{\xi}_a) \quad (9)$$

$$N_a(\vec{\xi}) = \frac{1}{8} (1 + \xi_a \xi)(1 + \eta_a \eta)(1 + \zeta_a \zeta) \quad (10)$$

Once the source densities at the quadrature points, $\vec{\xi}_l$, have been found, they are numerically integrated over the hex, using equations 11-15, to get the relative probability for that hex, $D_{i,j,k}$. The PDF, $P_{i,j,k}$, is found by

normalizing these $D_{i,j,k}$, such that $P_{i,j,k} = \frac{D_{i,j,k}}{N}$ and $N = \sum_{i,j,k} D_{i,j,k}$, and the CDF is the cumulative sum of

the PDF.

$$D_{i,j,k}(\vec{\xi}) \equiv \int_{-1}^1 g(\vec{\xi}) d\vec{\xi} \cong \sum_{l=1}^{n_{\text{int}}} g(\tilde{\xi}_l, \tilde{\eta}_l, \tilde{\zeta}_l) W_l \quad (11)$$

$$g(\vec{\xi}_l) = S(\vec{\xi}_l) j(\vec{\xi}_l) \quad (12)$$

$$j(\vec{\xi}_l) = \begin{vmatrix} x_\xi x_\eta x_\zeta \\ y_\xi y_\eta y_\zeta \\ z_\xi z_\eta z_\zeta \end{vmatrix} \quad (13)$$

$$x_\xi(\vec{\xi}_l) = \sum_{a=1}^8 N_{a,\xi}(\vec{\xi}_l) x_a^e \quad (14)$$

$$N_{a,\xi}(\vec{\xi}_l) = \frac{1}{8}(\xi_a)(1 + \eta_a\eta_l)(1 + \zeta_a\zeta_l) \quad (15)$$

The Jacobian determinant used here, $j(\vec{\xi}_l)$, is not related to the Jacobian used to map the plasma coordinates to real space, and represents the amount of real space per unit of space in the natural coordinate system.

The cell to be sampled is determined using a hierarchical linear search. A uniformly sampled random variable is compared against the CDF values in the last hex in each toroidal slice, the last hex in each radial ring of that toroidal slice, and finally the contiguous values for poloidal angle for each hex in the selected radial ring. Once the hex cell is identified a source location with the hex is found using rejection sampling. Three random variables are used to sample a point uniformly in the natural coordinates. The product of the source density and the Jacobian determinant, Sj , at this point in the natural coordinates is calculated using equations 8-10, and accepted if $\mu \cdot [S \cdot j](\vec{\xi}) \leq (S \cdot j)_{\max}$, where μ is a random variable sampled uniformly between 0 and 1. Thus the source locations within the hex are selected based on the first order variation of the source within the hex.

This method was applied to two different systems. The first problem used an ideal torus with a uniform source to verify the implementation of the method by comparison with a solution which can be easily calculated using MCNPX's built-in general source. The second system was the ARIES Compact Stellarator (ARIES-CS), which has a sufficiently complex geometry and source distribution to require this method. Previous work modeled the ARIES-CS source with a 0th-order predecessor to this method in which the relative probability of each hex was based on the volume of the hex and a simple average of the vertex source densities, and the source location inside the hex was sampled uniformly in the natural coordinate system [10]. The 1st-order method should allow a more accurate representation for a fixed number of flux surfaces, or a similar accuracy with fewer flux surfaces. In this work, the 1st-order results are first compared to a uniform source to demonstrate the need for such improved source representations. Then the 1st-order results are compared with 0th-order results, each generated using a large number of flux surfaces. With a fine mesh, the difference between 0th- and 1st-order results should be small, thus validating correctness of the 1st-order method for a geometrically distorted system.

Several metrics were used to evaluate the performance of this method. First the sampling efficiency of the 1st-order conformal hexahedral mesh method was computed with several different resolutions to investigate both the magnitude of the efficiency and how it changes with increased resolution of the mesh. It is expected that improving the mesh resolution will increase the efficiency. It should be noted that the 0th-order method will have a sampling

efficiency of 100% as no rejection is employed. Ratios of the source PDFs and the hex volumes were then compared as indicators of the differences between the 1st- and 0th- order sources. Finally, the NWLs of the 1st-order, 0th-order, and uniform source were compared.

3.1 Uniform Torus

The first test case was a finely segmented torus developed to verify the method implementation. A uniform source was generated with this new hex mesh method for a uniform torus with a 5 m major radius and a 1 m minor radius. These results were compared to those from a source defined using the SDEF card in MCNPX. The segmentation of the geometry, 288 surfaces on a quarter torus, enabled a detailed comparison of the neutron current across each surface.

The comparison of the results generated with the SDEF source and those generated with the new source provide confirmation that the new method is generating and sampling the source properly. The conformal hexahedral mesh source was generated using 80 flux surfaces, 60 toroidal increments, and 50 poloidal increments. To ensure small statistical error, 10^8 particles were used for each case. The ratio of the results was calculated for each of the surfaces. The average ratio was 0.9999 with a standard deviation of 2.5×10^{-3} and a maximum relative difference of 7.7×10^{-3} . An average ratio very close to 1 confirms that the normalizations were consistent. By propagating the statistical error of the results to the ratios, we find that the ratios had a maximum statistical error of 2.9×10^{-3} and an average statistical error of 2.4×10^{-3} . The standard deviation of the ratios is the same order of magnitude as the statistical error in the ratios, indicating that any discrepancies are dominated by statistical error. These metrics indicate that this 1st-order methodology is implemented correctly.

3.2 ARIES Compact Stellarator

The second test case was ARIES-CS, a stellarator with three field periods, an average major radius of 7.75 m, an average minor radius of 1.7 m, an aspect ratio of 4.5, and a fusion power of 2400 MW [8]. The neutron source volume of ARIES-CS can be seen in Figure 3. This system was originally analyzed using both a uniform source and a 0th-order source [8].

The sampling efficiency for the ARIES-CS problem ranged between approximately 75% and 85%. The sampling efficiency for each hex can be found by taking the ratio of S_j to $S_{j_{max}}$ for that hex. The overall sampling efficiency is the sum of these efficiencies weighted by the probability of selecting each hex. Changing the mesh resolution in the toroidal (srcDimT) and poloidal (srcDimP) directions improves the efficiency, but quickly approaches an asymptote so little improvement could be gained from further refinement (see Figure 4). Increasing

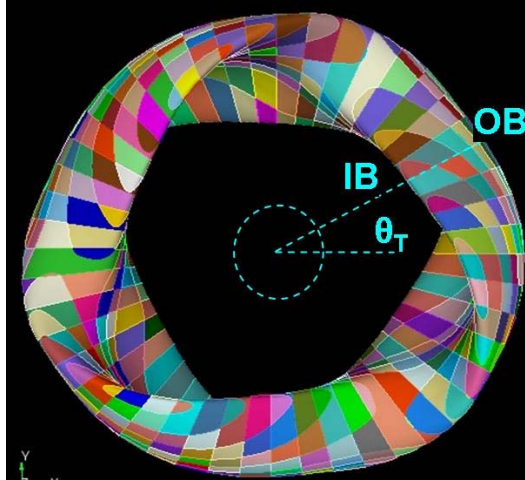


Figure 3. The source region for the ARIES-CS machine.

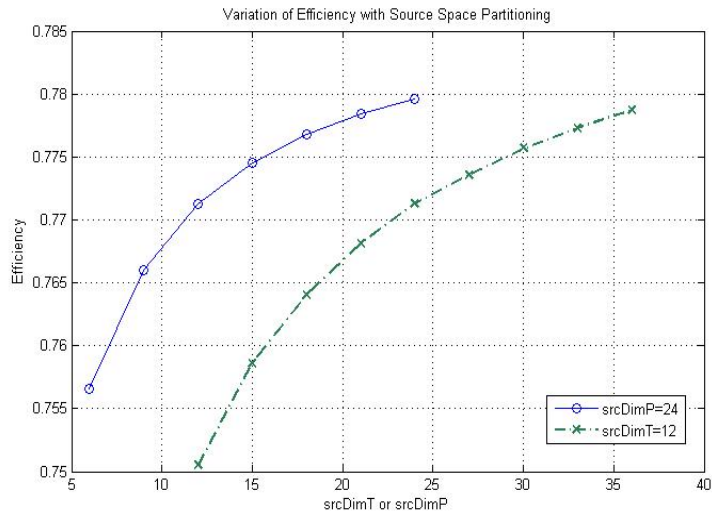


Figure 4. Conformal hexahedral mesh sampling efficiency as a function of toroidal (srcDimT) and poloidal (srcDimP) mesh refinement. 49 flux surfaces were used.

the number of flux surfaces improved efficiency as well, but also approached an upper bound. When 12 toroidal and 24 poloidal increments were used the efficiency with 49 surfaces was 0.7713, with 98 surfaces was 0.8482, and with 147 surfaces was 0.8772. In general, increasing the number of increments of the source definition increases the source sampling efficiency, but good (i.e. > 80%) efficiency can be obtained without an unwieldy number of increments.

The ratio of the 1st-order to 0th-order source PDFs ranged from 0.9562 to 1.0082 and the ratio of the volumes ranged from 0.9539 to 1.0104. These ratios were taken from data using 49 flux surfaces, 12 toroidal increments and 24 poloidal increments. When the resolution was increased to 147 flux surfaces, 24 toroidal increments and 48

poloidal increments the range of the source PDF ratio became 0.9863 to 1.0025 and that of the volumes became 0.9839 to 1.0029. The 1st-order method calculated slightly higher values for both the source and the volume on the outboard portion of the plasma and lower values toward the magnetic axis. The difference between the source densities computed by the 1st-order and the 0th-order was not large (<5% for 49 flux surfaces and <2% for 147 flux surfaces), but depending on the resolution of the source mesh, could have an important impact on NWL. As coarser meshes are used the difference between the PDFs becomes more pronounced and the resulting difference in analysis will become correspondingly more pronounced.

A uniform volume source is the most rudimentary source distribution that could be used for ARIES-CS, and previous work has demonstrated the inadequacies of this model for a 3-D neutronics calculation [8]. The conformal hexahedral mesh source distribution was generated on 147 flux surfaces and the uniform on 49 flux surfaces. Each distribution had 24 toroidal increments and 48 poloidal increments. One third of the geometry was segmented into 352 surfaces for detailed analysis. The ratio of the 1st-order NWL to uniform NWL ranged between 0.2445 and 1.914. The average ratio was 0.9789 with a standard deviation of 0.365 and an average relative error of 5.4×10^{-3} . Even though 10^8 particles were used, 4 surfaces were excluded from the analysis due to high statistical error. These surfaces had very small areas so their contribution to the total NWL is quite small and their implication for the comparison is therefore insignificant. A plot of the relative difference between the 1st-order and uniform results against the 1σ statistical error is shown in Figure 5, with lines showing the points where the relative differences are 1, 2 and 3 times the statistical error. Almost all data points are above the 3σ line indicating that the results are statistically different. A comparison between the 0th-order and uniform NWLs has the same trend. These results confirm that the uniform case is not a good approximation to the real source and the use of higher order methods will be more accurate.

The 0th-order method was introduced as an improvement upon the uniform source distribution. The ratio of the 1st-order NWL to 0th-order NWL ranged between 0.9793 and 1.019. The average ratio was 0.9998 with a standard deviation of 7.4×10^{-3} and an average relative error of 6.5×10^{-3} . Both of these sources were created with 147 flux surfaces, 24 toroidal increments and 48 poloidal increments. Again 10^8 particles were used and the same 4 surfaces were excluded due to error. A plot of the relative difference between the 1st-order and 0th-order results against the 1σ statistical error is shown in Figure 6. The bulk of data points all fall within 1σ , almost all within 2σ , and all but one within 3σ . This indicates that there is little statistically significant difference between the 1st and 0th-order results and thus confirms that the 1st-order case is correct in distorted geometries, which are the cases of interest for this method.

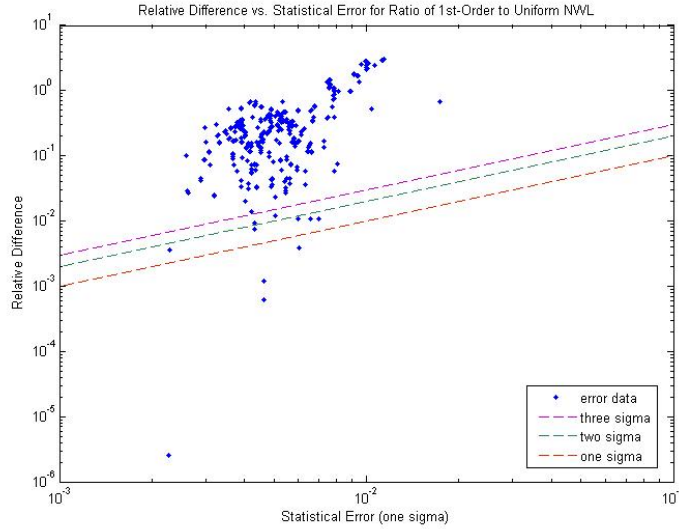


Figure 5. Relative difference between the 1st-order and Uniform vs. the statistical error of the ratio. One, two, and three sigma boundary lines are shown.

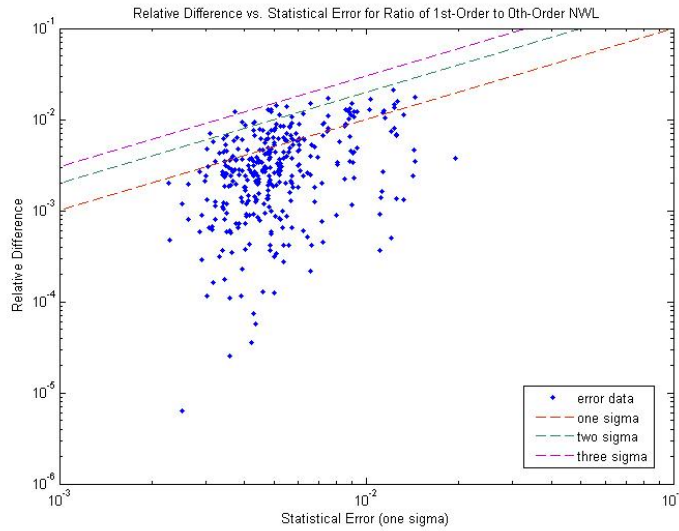


Figure 6. Relative difference between the 1st-order and 0th-order vs. the statistical error of the ratio. One, two, and three sigma boundary lines are shown.

While the intent here was to show that with a fine mesh the 1st- and 0th-order methods are consistent, it is not always convenient to use such high resolution. In the case of coarser meshes it is anticipated that the 1st-order case will be superior to the 0th-order case. The 1st-order method will more accurately calculate the hex source PDF and, more importantly, it will allow better sampling of each hex through the rejection sampling method that accounts for source variations within the hex. A limiting case illustration of this would be when using only one flux surface. In

this scenario the 0th-order would simply be a uniform case while the 1st-order would capture some source variation. Future work will be to perform studies in which the number of flux surfaces is varied, illustrating the differences between the 1st- and 0th-order methods.

The application of this method to the ARIES-CS machine illustrated that the conformal hexahedral mesh can be used for geometries and sources which are sufficiently complex to prohibit accurate source definition using standard MCNPX methods. The comparison of this method with a uniform source motivates why a better source is required and a comparison with a 0th-order source confirms that the 1st-order method can correctly capture the source behavior.

4. Summary and Conclusions

This paper described two different representations of neutron source distributions for use in high fidelity three-dimensional neutronics analyses of complex geometries for fusion energy systems. This work was motivated by the increased importance of the effects of the neutron source distribution which has been driven by the ability to use CAD-based continuous energy Monte Carlo calculations in combination with high resolution output. These methods capture spatial variation of the source better than previous approximate representations and can be closely coupled to the results of plasma physics simulations.

The cylindrical mesh method can be used for toroidally symmetric machines, such as tokamaks and spherical tori, and uses the standard “geqdsk” format for plasma source information. This method uses a quadrilateral grid and samples the source uniformly in R and Z, and then uniformly in toroidal angle. The conformal hexahedral mesh method can be applied to more complicated machines, such as stellarators, and uses plasma source data generated in an idealized toroidal coordinate system. This method uses a structured hexahedral mesh and samples the source in a manner which captures first-order variations of the source within each hex element. Each method was used to analyze a representative real machine where neutron wall loading was used as the basis for the comparisons.

The cylindrical mesh method was applied to the ARIES-RS machine which demonstrated that using a source generated by this method instead of a standard Monte Carlo source is necessary. While a source that is well defined using the MCNP general source, like the three region source used in the past, is capable of capturing many of the effects of the real source in some cases, it may not be accurate enough for detailed calculations in general. In ARIES-RS, the disagreement for the inboard results ($\pm 10\%$) suggests that the source from the cylindrical mesh method should be used in future analysis.

The conformal hexahedral mesh was applied to both a uniform torus and the ARIES-CS machine. Because the hexahedral mesh method results matched the standard MCNPX results for the uniform torus, it can be concluded that this new method is valid. The analysis of ARIES-CS showed that reasonable sampling efficiency can be obtained without requiring a highly refined source mesh. The source density and volume of each hex calculated by the 0th-order and 1st-order methods approach one another as the source mesh is refined. Comparison of the conformal hexahedral mesh method with a uniform source in ARIES-CS highlighted the need for good source definitions. Examining the new method with respect to a 0th-order method for a finely resolved source further verified that the conformal hexahedral mesh method is correct in complex geometries. Overall, this case illustrated that this method can be used for complicated geometries and that it should be used when detailed engineering parameters, such as neutron wall loading, are needed accurately. Future work will investigate the distinction between when the 0th-order method is sufficient and when the 1st-order method would be desirable.

As a secondary benefit, both of these source modelling strategies provide a mechanism for more tightly binding the neutronics calculations to the plasma physics simulations. The neutronics codes can be adapted to directly read the plasma physics simulation output, whether the *geqds* format or the set of coefficients for a 3-D Jacobian transformation. This has a benefit during design iterations where changes to the machine design can impact the plasma conditions and the source distribution.

These new source generation methods are an improvement over previous source models for fusion energy systems. They are able to capture the true source behavior more accurately and can be closely coupled with plasma physics codes. For these reasons the new methods should be used for high resolution neutronics calculations in toroidal fusion machines.

Acknowledgements

This work was supported, in part, by the United States Department of Energy's Office of Fusion Energy Sciences, under project DE-FG02-98ER54462. The authors would also like to thank Charles Kessel (PPPL) for providing ARIES-RS plasma information and Drs. Long-Poe Ku (PPPL) and James Lyon (ORNL) for providing ARIES-CS plasma information.

References

- [1] Sawan, M.E., L.A. El-Guebaly, "Neutronics and shielding results of the U.S. ITER blanket trade-off study," *Fusion Engineering and Design*, **28**, pp 551 (1995).
- [2] Smith, B., P. Wilson, M. Sawan, T. Bohm, "Source Profile Analysis for the ITER First Wall/Shield Module 13," Accepted by *Fusion Science and Technology* as proceedings of the 18th TOFE Conference.
- [3] Smith, B., P.P.H. Wilson, M.E. Sawan, "Three Dimensional Neutronics Analysis of the ITER First Wall/Shield Module 13," Proceedings of 22nd IEEE/NPSS Symposium of Fusion Engineering, Albuquerque, NM, June 2007.
- [4] Bosch, H.S., G.M. Hale, "Improved formulas for fusion cross-sections and thermal reactivities," *Nuclear Fusion*, **32** (1992).
- [5] EFIT Equilibrium/Fitting Code, 06/03/2006, General Atomics, August 2008, http://fusion.gat.com/THEORY/efit/index.html_new.
- [6] El-Guebaly, L.A., The ARIES Team, "Overview of ARIES-RS neutronics and radiation shielding: key issues and main conclusions," *Fusion Engineering and Design* **38** (1997) 139-158.
- [7] Hughes, G.H., et al., *MCNPX User's Manual Version 2.4.0*, LA-CP-02-408, Los Alamos, NM, Los Alamos National Laboratory, 2002.
- [8] El-Guebaly, L., et al., "Designing ARIES-CS Compact Radial Build and Nuclear System: Neutronics, Shielding, and Activation," *Fusion Science and Technology* 54.3 (2008) 747-770.
- [9] Personal Communication with Jim Lyon, Oak Ridge National Laboratory (May 2006).
- [10] MHD Equilibrium and Stability Codes, (1) VMEC, Oak Ridge National Laboratory, FED, 20 Nov. 2008, http://www.ornl.gov/sci/fed/Theory/stci/code_library.html#VMEC.
- [11] Hughes, T.J.R., The Finite Element Method: Linear Static and Dynamic Finite Element Analysis, Dover, 2000.